A R C H I V E S O F M E T A L L U R G Y A N D M A T E R I A L S
Volume 53 2008 Issue 1

M. WITKOWSKA*, W. RATUSZEK*, J. RYŚ*, A. ZIELIŃSKA-LIPIEC*, K. CHRUŚCIEL*

THE EFFECT OF DEFORMATION AND ANNEALING ON SIGMA PHASE PRECIPITATION IN DUPLEX STEELS

WPŁYW ODKSZTAŁCENIA I WYŻARZANIA NA WYDZIELANIE FAZY SIGMA W STALACH DUPLEX

The present work concerns the influence of deformation and annealing conditions on sigma phase precipitation in two model ferritic-austenitic steels of duplex type X1CrNi24-6 and X4CrNiMo24-6-2. After the preliminary thermo-mechanical treatment both steels were subjected to cold rolling up to 70% and 90% of reduction and subsequent annealing within the temperature range 600-800°C for various time. X-ray investigations included the phase analysis and texture measurements of the component phases, i.e. austenite (γ), ferrite (α) and sigma phase (σ). Microstructure observations were conducted by means of optical, scanning and electron microscopy. The results of texture and microstructure analysis indicate that the mechanisms of sigma phase precipitation; $\alpha \rightarrow \sigma$ and $\alpha \rightarrow \sigma + \gamma'$, depend on chemical composition and degree of deformation as well as temperature and time of annealing.

Keywords: ferritic-austenitic steel, sigma phase, precipitation processes, two-phase structure

Prezentowana praca dotyczy analizy wpływu odkształcenia i warunków wyżarzania na wydzielanie fazy sigma w dwóch modelowych stalach ferrytyczno-austenitycznych typu duplex X1CrNi24-6 i X4CrNiMo24-6-2. Obie stale po wstępnej obróbce cieplno-mechanicznej poddano walcowaniu na zimno do 70% i 90% odkształcenia a następnie wyżarzano w zakresie temperatur 600-800°C w różnym czasie. Badania rentgenowskie obejmowały analizę fazową, pomiary tekstur składowych faz: austenitu, ferrytu i fazy sigma. Obserwacje mikrostruktury przeprowadzono przy użyciu mikroskopu świetlnego, skaningowego i elektronowego. Wyniki tekstury i analiza mikrostruktury wskazują na to, że mechanizm wydzielania fazy sigma $\alpha \rightarrow \sigma$ i $\alpha \rightarrow \sigma + \gamma'$ zależy od składu chemicznego, stopnia odkształcenia jak również temperatury i czasu wyżarzania.

1. Introduction

Duplex steels exhibit favourable combinations of mechanical properties and corrosion resistance in comparison to one phase austenitic and ferritic stainless steels [1]. Very important from the view point of the most important properties of these steels are the precipitation processes of intermetallic phases, especially sigma phase, which usually nucleates within the temperature range above 600°C up to 900–950°C in the case of high-alloy steels. Sigma phase shows complex tetragonal structure, comprising 30 atoms in unit cell, which are arranged in layers. The process of sigma phase precipitation proceeds either by direct nucleation from ferrite ($\alpha \rightarrow \sigma$) or through the eutectoid decomposition of ferrite into sigma phase and secondary austenite ($\alpha \rightarrow \sigma + \gamma'$) [2–7]. The results of number of investigations indicate that the mechanisms of sigma phase precipitation strongly depend on chemical composition, as well as deformation and annealing conditions [8–11]. In chromium steels sigma phase has composition Fe-Cr and usually precipitates within the temperature range below 820°C [8,12]. On the other hand formation of sigma phase in high alloyed steels, containing additionally for example molybdenum and tungsten, is shifted to higher temperatures since tendency to σ-phase precipitation results from joined influence of chromium and the other elements [2–4]. Simultaneously constitution of sigma phase in high alloy steels is more complex, for example (CrM)Fe. The technological processes for duplex steel production include usually hot-deformation with intermediate and/or subsequent annealing followed by cold-deformation. That is why it is very important to determine the influence of deformation and annealing conditions on σ-phase precipitation in duplex type steels with different chemical compositions.

* DEPARTMENT OF PHYSICAL AND POWDER METALLURGY, AGH - UNIVERSITY OF SCIENCE AND TECHNOLOGY, 30-059 KRAKÓW, AV. MICKIEWICZA 30, POLAND

TABLE 1

Chemical composition of two-phase steels (in wt.%)

Steel	Cr	Ni	Mo	C	N	Mn	Si	S	P	Al
A	23.7	6.0	0	0.009	0.0122	1.23	0.34	0.01	<0.008	<0.02
B	24.3	6.44	1.57	0.04	0.014	1.29	1.02	0.013	<0.009	0.009

2. Material and experimental procedure

The materials investigated in the present research were two model stainless steels of duplex type, X1CrNi24-6 (steel A), and X4CrNiMo24-6-2 (steel B), with the chemical compositions given in Table 1. In both steels the volume fraction of ferrite and austenite were estimated at $V_f \sim 60\%$, $V_a \sim 40\%$. That is why the ferritic α-phase was more continuous and constituted the matrix with islands of the austenitic γ-phase.

The steel ingots were industrially homogenized and hot-worked at the temperatures 900–1000°C. Further processing included solution treatment, that is annealing at temperature 1100°C for 3–6 hours with subsequent quenching in the water. After the preliminary thermo-mechanical treatment the steels were subjected to reversed rolling at the room temperature within the range up to 70% and 90% of thickness reduction. Following the process of cold-rolling the specimens were annealed at temperatures 600°C, 700°C and 800°C for 30 minutes, 1 and 10 hours with subsequent water quenching.

X-ray investigations were conducted by means of Bruker diffractometer D8 Advance, using Co K_α radiation ($\lambda_{K\alpha}$ = 1.79 Å). X-ray examination included the texture measurements and the phase analysis from the centre layers of the sheets. The incomplete pole figures were recorded of three planes for each of the component phases, namely; {111}, {200}, {220} planes for austenite and {110}, {200}, {211} for ferrite. In the case of sigma phase the {420}, {410}, {331} and {411} pole figures were measured. Microstructure observations were carried out from the longitudinal sections (ND-RD) of the sheets by means of Leica optical microscope, Stereo-Scan scanning microscope and JEM200CX electron microscope.

3. Results

The results of the X-ray diffraction analysis for both examined steels are presented in figures 1, 2 and 7, 8. Measurements of the orientations distribution sigma phase are given in the form of pole figures 6, 10 and 11. The microstructure observations (Figs. 3–5, 9) are concentrated on the analysis of the σ-phase precipitation. From all the microstructure examination it results that sigma phase precipitation proceeded within the temperature range 600–800°C in the steel A and above 800°C in the steel B.

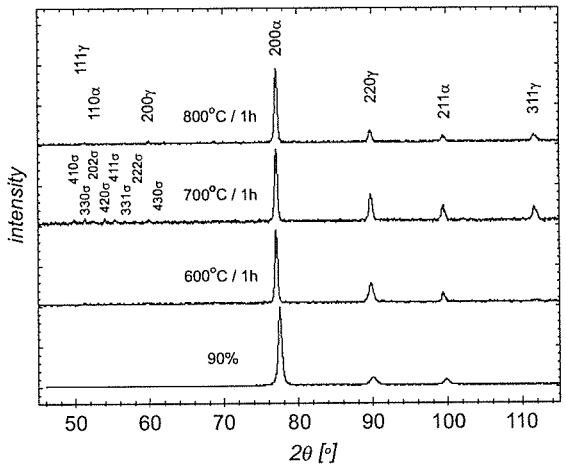

Fig. 1. Difraction patterns after 90% of rolling deformation and annealing at temperature from the range 600–800°C for 1 hour for steel A

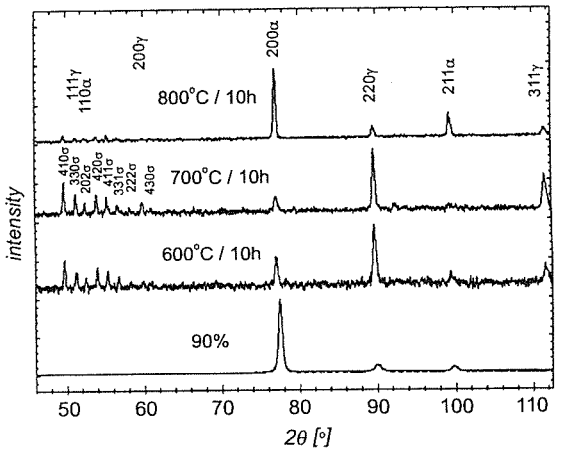

Fig. 2. Difraction patterns after 90% of rolling deformation and annealing at temperature from the range 600–800°C for 10 hours for steel A

In the case of steel A (i.e. without Mo addition) the strongest diffraction effects concerning σ-phase precipitation were observed after annealing at the temperature 700°C for 10 hours (Fig. 2). For the applied temperature range the strongest diffraction peaks for sigma phase were 410σ and 420σ. With increasing annealing

temperature a decrease of orientation density was observed in ferrite especially from {100} planes parallel to the rolling plane. It is assumed that the weakening of the ferrite texture is the result of the σ-phase precipitation. On the other hand prolongation of the annealing time from 1 hour to 10 hours caused an increase in the intensity of 220γ and 311γ austenite peaks. Such an effect presumably indicates at eutectoid decomposition of ferrite into the sigma phase and secondary austenite ($\alpha \rightarrow \sigma + \gamma'$).

Microstructure observations (Figs. 3–5) conducted after 70% and 90% of rolling reduction and subsequent annealing at 700°C show the effect of deformation degree on the mechanism of σ-phase nucleation. In the case of specimens after 70% reduction the precipitates of sigma phase were observed mainly along deformation bands (Fig. 3a) whereas in specimens deformed up to 90% of rolling reduction the arrangement of sigma phase precipitates is parallel to the rolling plane seems like along the ferrite/austenite interphases (Fig. 4). The amount of σ-phase was obviously increasing with the annealing time, since the precipitates were growing deep into the ferrite areas [13].

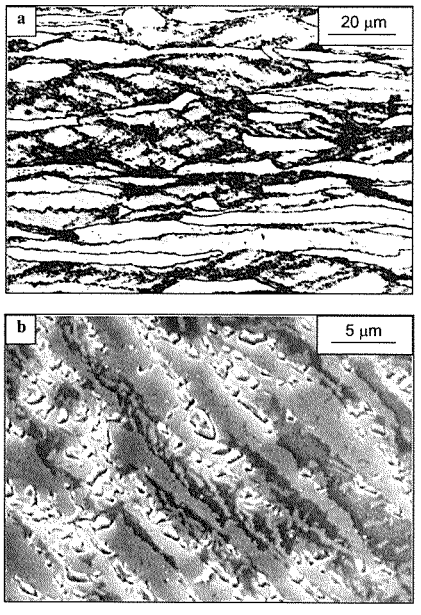

Fig. 3. Microstructures of the steel A after 70% reduction and annealing at: (a) 700°C/30' optical microscope and (b) 700°C/2h scanning microscope

The analysis of the σ-phase texture was carried out based on the (410) and (420) pole figures. Figures 6a and b present the texture of σ-phase for the case of steel A after annealing within the temperature range 600–800°C for 1 and 10 hours. The character of pole figures was similar for all the applied annealing temperatures. After annealing for 1 hour (Fig. 6a) the (001) planes were parallel to the rolling plane, whereas prolongation of annealing up to 10 hours (Fig. 6b) resulted in the change of the orientation. The texture exhibited the maximum intensity for (420) and (410) planes i.e. in the centre of the pole figures, which indicate at the fibre character of the sigma phase texture.

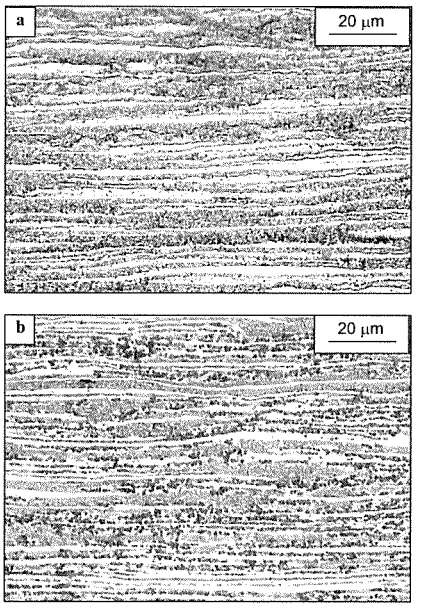

Fig. 4. Microstructures of the steel A after 90% reduction and annealing at: (a) 700°C/30' and (b) 700°C/2h optical microscope

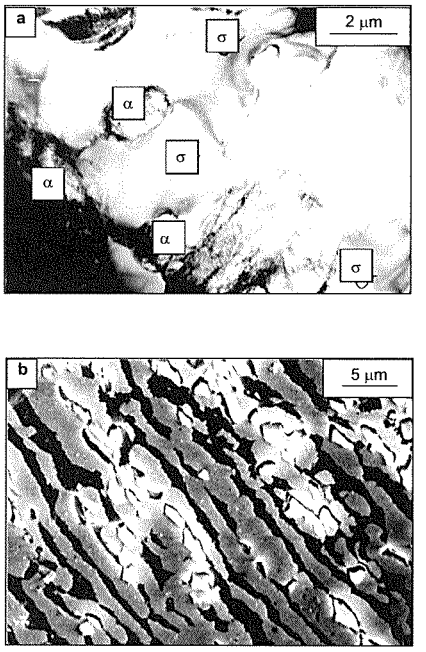

Fig. 5. Microstructures of the steel A after 90% reduction and annealing at: (a) 700°C/10h electron microscope and (b) 800°C/10h scanning microscope

The results of X-ray diffraction analysis for steel B (with 1.5%Mo addition) are given in figures 7 and 8. The strongest diffraction effects concerning the σ-phase were observed after annealing at the temperature 800°C

for 1 hour. The appearance of sigma phase caused significant weakening or decay of the 200α and 211α peaks from ferrite, indicating at complete decomposition of the α-phase. Simultaneously the intensity of the 220γ, 200γ and 311γ austenite peaks considerably increased. Both effects seem to indicate at the eutectoid decomposition of ferrite into σ-phase and secondary austenite ($\alpha \rightarrow \sigma + \gamma'$). Comparison of diffraction pattern for steels A and B registered at 800°C/1h/10h indicates at relatively high amounts of σ-phase within the structure of steel B and very small amount (almost absence) of σ-phase in the case of steel A.

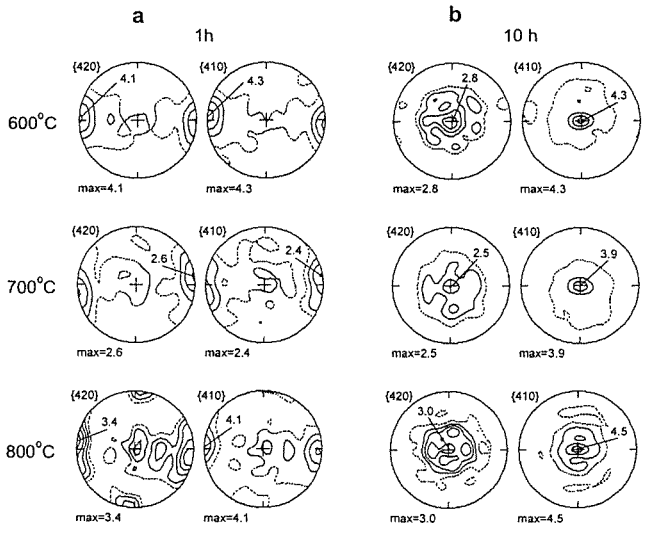

Fig. 6. Pole figures {420} and {410} of the σ-phase for steel A after 90% of deformation and annealing at 600°C, 700°C and 800°C for: (a) 1 hour and (b) 10 hours

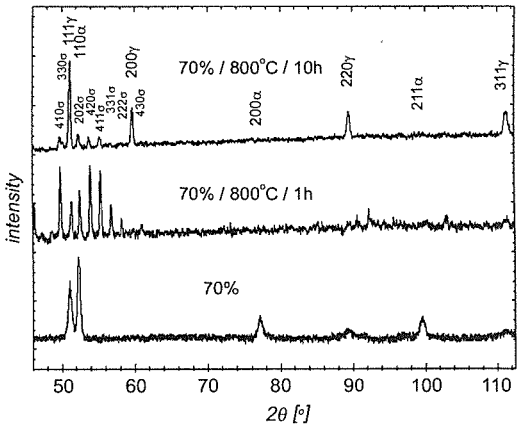

Fig. 7. Diffraction patterns after 70% of rolling deformation and annealing at temperature 800°C for 1 hour and 10 hours for steel B

Microstructure observations (Fig. 9) confirmed the precipitation of sigma phase along entire width of ferrite bands. The process of σ-phase precipitation led to the appearance of areas depleted in ferrite stabilizing elements, i.e. chromium and molybdenum, resulting in formation of the secondary austenite ($\alpha \rightarrow \sigma + \gamma'$) [14, 15]. In the case of steel B after 70% and 90% of deformation and annealing at the temperature 800°C the major components of the σ-phase texture remained unchanged regardless of the annealing time. The only changes concern the texture intensity (Fig. 10). In all the analysed cases the maximum intensity appeared in the centre of the (420) and (410) pole figures indicating at fibre character of the texture.

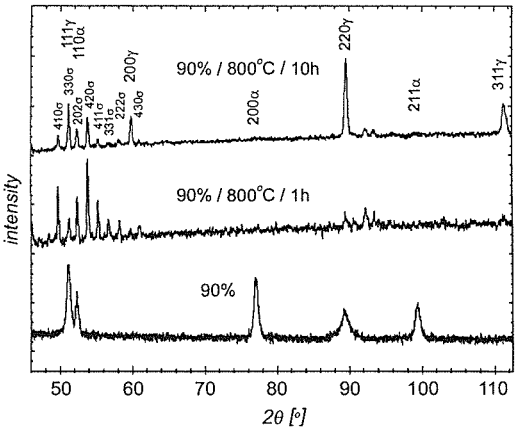

Fig. 8. Diffraction patterns after 90% of rolling deformation and annealing at temperature 800°C for 1 hour and 10 hours for steel B

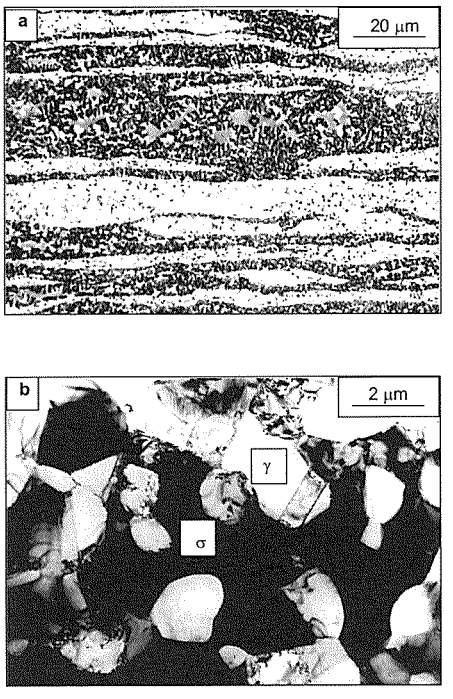

Fig. 9. Microstructures of the steel B after 70% reduction and annealing at 800°C/2: (a) optical microscope and (b) electron microscope

Diffraction patterns in figures 1, 2, 7 and 8 show that the peaks $\{110\}\alpha$ for ferrite and $\{202\}\sigma$ for the sigma phase are overlapping. Comparison of the pole figures $\{110\}\alpha$ and $\{110\}\alpha+\{202\}\sigma$ (Fig. 11) indicates at marked similarity of both figures in steel A and clear differences for the case of steel B.

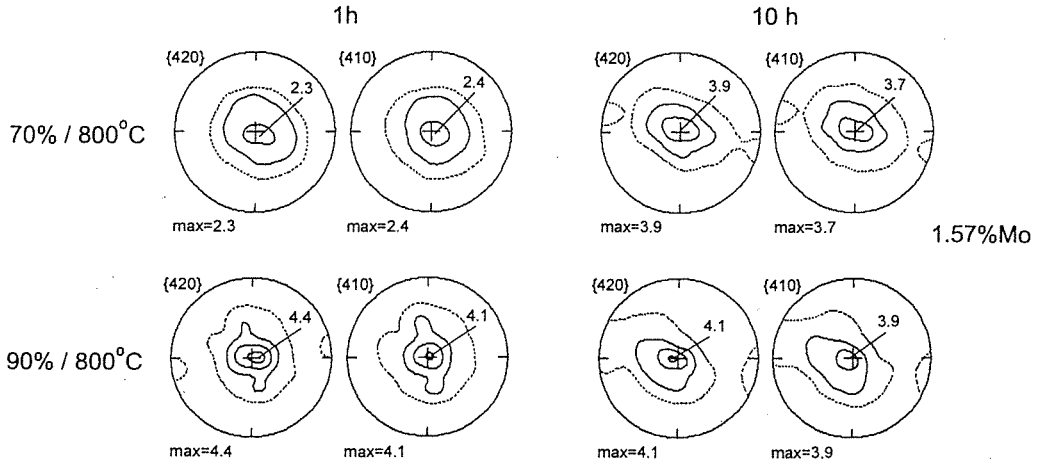

Fig. 10. Pole figures {420} and {410} of the σ-phase for steel B after 70% and 90% of deformation and annealing at 800°C for 1 and 10 hours

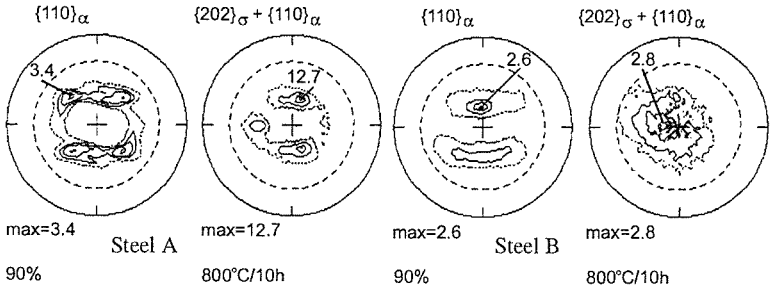

Fig. 11. Pole figures {110} of ferrite after 90% reduction and {110}α+{202}σ of ferrite and sigma phase after annealing at 800°C/10h for steel A and steel B

The comparison of the ferrite {110} pole figure after 90% of deformation with the {202}σ+{110}α pole figure after annealing at 800°C indicates that ferrite completely decomposed into σ-phase and secondary austenite (Fig. 11). It is suggested that in the case of steel B (with 1.5% Mo addition) the process of sigma phase precipitation proceeds entirely through the decomposition of ferrite. However in the case of steel A (without Mo) a contribution of both mechanisms is possible i.e. direct precipitation from ferrite and eutectoid decomposition of ferrite.

4. Concluding remarks

Microstructure examination indicates that plastic deformation favors the nucleation of σ-phase and the preferential sites for sigma phase precipitation after 70% of reduction are deformation bands within the ferrite areas. However at very high deformation degrees (ex. 90% reduction) the sigma phase precipitation proceeds along the α/γ phase boundaries, which are arranged parallel to the rolling plane.

Based on the analysis of the orientation distribution and microstructure observations it is concluded that the dominant mechanism of sigma phase precipitation in both steels is the ferrite decomposition ($\alpha \rightarrow \sigma + \gamma'$). However a certain contribution of the mechanism of direct precipitation from ferrite ($\alpha \rightarrow \sigma$) is not excluded in the case of steel A. Additionally, the texture analysis indicates at the preferential precipitation of sigma phase, which exhibits the fibrous character of its texture.

Analysis of diffraction patterns indicates that chemical composition affects the temperature range for sigma phase nucleation. In the case of steel A the strongest diffraction effects concerning σ-phase precipitation were observed after annealing at the temperature 700°C for 10 hours. In the case of steel B containing 1.5% of molybdenum strong diffraction effects due to sigma phase were

still observed after annealing at the temperature 800°C. The precipitation of sigma phase is shifted towards higher temperatures due to presence of molybdenum within the composition of steel B.

Acknowledgements

The work was supported by the Polish Committee for Scientific Research (KBN) under the contract No.11.11.110.712.

REFERENCES

[1] M. Pohl, O. Storz, T. Glogowski, Effect of intermetallic precipitations on the properties of duplex stainless steel, Materials Characterization **58**, 65 (2007).

[2] W. Reick, M. Pohl, A.F. Padilha, Recrystallization-Transformation Combined Reactions during Annealing of a Cold Rolled Ferritic-Austenitic Duplex Stainless steel, ISIJ International **38**, 6, 567 (1998).

[3] J.-O. Nilsson, Super duplex stainless steels, Materials Science and Technology **8**, 685 (1992).

[4] J.K.L. Lai, K.W. Wong, D.J. Li, Effect of solution treatment on the transformation behavior of cold-rolled duplex stainless steel, Materials Science and Engineering A **203A**, 356 (1995).

[5] C.H. Shek, K.W. Wong, J.K.L. Lai, Review of temperature indicators and the use of duplex stainless steels for life assessment, Materials Science and Engineering **R19**, 153 (1997).

[6] T.H. Chen, J.R. Yang, Effects of solution treatment and continuous cooling on σ-phase precipitation in a 2205 duplex stainless steel, Materials Science and Engineering **A 311**, 28 (2001).

[7] Y. S. Han, S. H. Hong, Microstructural Changes during Superplastic Deformation of Fe-24Cr-7Ni--3Mo-0.14N Duplex Stainless Steel, Materials Science and Engineering **A 266**, 276 (1999).

[8] J. Barcik, Proces wydzielania fazy sigma w chromowo-niklowych stalach austenitycznych, Prace naukowe Uniwersytetu Śląskiego 340, Katowice (1979).

[9] A.F. Padilha, W. Reick, F.C. Pimenta, Untersuchung zum verleich der σ-phasenausscheidung in einem rostfreien superferrit und einem duplex-stahl, Z. Metallkd. **92**, 351 (2001).

[10] K. Ravindranath, S.N. Malhora, The influence of aging on the intergranular corrosion of 22 chromium-5 nickel duplex stainless steel, Corrosion Science **37**, 1, 121 (1995).

[11] Y.S. Ahn, J.P. Kang, Effect of aging treatments on microstructure and impact properties of tungsten substituted 2205 duplex stainless steel, Materials Science and Technology **16**, 382 (2000).

[12] J.R. Davies, Alloy Digest Sourcebook Stainless Steels ASM (2000).

[13] M. Witkowska, W. Ratuszek, J. Ryś, A. Zielińska-Lipiec, Faza sigma w stalach ferrytyczno-austenitycznych, Problemy współczesnej techniki w aspekcie inżynierii i edukacji, Kraków 75, (2005).

[14] J. Ryś, W. Ratuszek, M. Witkowska, Analiza strukturalna wyżarzanych blach ze stali 0H24N6Mo1.5 typu duplex, Hutnik **7-8**, 414 (2004).

[15] M. Witkowska, W. Ratuszek, J. Ryś, A. Zielińska-Lipiec, Factors affecting annealing textures in duplex type steels, Applied Crystallography: Proceedings of the XIX Conference, Kraków, 185 (2004).

Received: 3 December 2007.